Biomaterials Science

mRNA delivery using non-viral PCL nanoparticles

Journal:	*Biomaterials Science*
Manuscript ID:	BM-ART-07-2014-000242.R1
Article Type:	Paper
Date Submitted by the Author:	30-Jul-2014
Complete List of Authors:	Palamà, Ilaria Elena; CNR Institute Nanoscience, Cortese, Barbara; CNR Institute Nanoscience, D'Amone, Stefania; CNR Institute Nanoscience, Gigli, Giuseppe; CNR Institute Nanoscience, ; Dept. Matematica e Fisica 'Ennio De Giorgi', University of Salento; Italian Institute of Technology (IIT), - Center for Biomolecular Nanotechnologies

Biomaterials Science

RSCPublishing

ARTICLE

mRNA delivery using non-viral PCL nanoparticles

Cite this: DOI: 10.1039/x0xx00000x

Ilaria E. Palamà,[a*] Barbara Cortese,[a] Stefania D'Amone,[a] and Giuseppe Gigli,[a,b,c]

Received 00th January 2012,
Accepted 00th January 2012

DOI: 10.1039/x0xx00000x

www.rsc.org/

Messenger RNA (mRNA) provides a promising alternative to plasmid DNA as a genetic material for delivery in non-viral gene therapy strategies. However, it is difficult to introduce mRNA *in vivo* mainly because of the instability of mRNA under physiological conditions. Here, mRNA-protamine complexes encapsulated poly(ε-caprolactone) (PCL) nanoparticles (NPs) are proposed for the intracellular delivery of mRNA molecules. The nanoparticles with a size of about 247 nm in diameter has a core-shell structure with mRNA-containing inner core surrounded by PCL layer, providing the high stability and stealth property to the nanoparticles. The partial neutralization of the negatively charged mRNA molecules with the cationic protamine allows one to modulate the release kinetics in the pH-dependent manner. At pH 7.4, mimicking the conditions found in the systemic circulation, only the 25% of mRNA is released after 48 hours post incubation; whereas at pH 5.0, recreating the cell endosomal environment, about 60% of the mRNA molecules are released within the same time window post incubation. These NPs show no cytotoxicity on NIH 3T3 fibroblasts, HeLa cells and MG63 osteoblasts up to 8 days of incubation. Given the stability, preferential release behavior, and well-known biocompatibility properties of PCL nanostructures, our non-viral PCL nanoparticles are a promising system that simultaneously resolved the two major problems of mRNA introduction and the instability, opening the door to various new therapeutic strategies using mRNA.

Introduction

Failure of clinical trials of non-viral vector-mediated gene therapy arises primarily from either an insufficient transgene expression level or immunostimulation concerns caused by the genetic information carrier. Neither of these issues could be addressed through engineering sophisticated gene delivery vehicles. As a rapidly emerging class of nucleic acid therapeutics, there are key benefits in using mRNA that is frequently applied as a gene delivery molecule in the fields of inherited genetic disorders, cancer immunotherapy and stem cell-based biomedical research as an alternative to plasmid DNA (pDNA)[1,2,3]. As a direct source of gene products, mRNA has several advantages, in first, mRNA contains no viral promoters (e.g. CMV) and bacterial sequences that can cause toxicity. Second, mRNA does not integrate into host genome, which may lead to deleterious mutation[4]. Third, gene expression via mRNA is relatively transient and therefore safer to use compared with DNA. Last but not least, as mRNA does not need to cross the nuclear envelop, it increases the chances of successfully transfecting quiescent cells. Indeed, mRNA can mediate a higher level of protein expression *in vivo* compared with DNA over shorter durations[5]. Moreover, the cytoplasmic delivery of mRNA circumvented the nuclear envelope, which resulted in a higher gene expression level. A variety of nanoparticles as non-viral systems have been investigated for the effective *in vivo* delivery of gene. These include lipid-based and polymer-based nanoparticles where the polynucleotides are encapsulated within the hydrophilic core or adsorbed on the cationic surface. In polymeric complexes, the negatively charged acid nucleic molecules could be easily attached by surface-absorption on cationic polymers and surfactants[6,7,8,9] or entrapped in the NP hydrophilic core prepared by double emulsion solvent evaporation methods[10,11]. An attractive polymer for mRNA application is the poly(ε-caprolactone) (PCL), approved by the Food and Drug Administration (FDA). Nanoparticles composed of PCL are promising for their high colloidal stability in biological fluid, facile cellular uptake by endocytosis, low toxicity *in vitro* and *in vivo*, and controlled release of their cargo[12].

Therefore, we propose a new non-viral nanosystem for delivery of mRNA as an alternative to plasmid DNA in gene therapy. In this work, as proof of concept, PCL nanoparticles have been developed as non-viral vector for the delivery of GFP-mRNA. The PCL NPs, obtained by the emulsion-diffusion-evaporation method, comprise a hydrophilic core with the active agent, a PCL shell, and a PVA coating to increase the colloidal stability. Prior to particle assembly, GFP-mRNA RNA molecules are reacted with protamine (PRM), a polycation widely used in drug[13,14] and gene delivery, to form an almost neutral mRNA-protamine complex. This leads to higher loading, better stability, and controlled release of the mRNA over time. In particular, protamine is an arginine-rich peptide with strong basic charge and it is a FDA approved nontoxic cationic peptide for use in humans as a heparin antagonist and as a long-acting delivery system for insulin. Protamine is also an excellent DNA condenser for *in vitro* cationic lipid-mediated gene transfer[15].

The physicochemical properties of the NPs are characterized by using various characterization techniques. The loading efficiency and release kinetics are analysed under different physiological conditions. The expression efficiency of mRNA

is studied *in vitro* on transfected NIH 3T3 fibroblasts, HeLa cells and MG63 osteoblasts.

Experimental

Materials and Methods

All tissue culture media and serum were purchased from Sigma-Aldrich, cell lines were purchased from American Tissue Type Collection (ATTC). The suppliers of the chemicals were as follows and were supplied by Sigma-Aldrich: thiazolyl blue tetrazolium bromide (MTT), phosphate buffered saline (PBS), Fluoroshield with DAPI, protamine sulphate Poly-(-caprolactone) (PCL) with an average molecular weight (MW) of 14.800 Da, Polyvinyl alcohol (PVA, MW 13-23 kDa, 87–80% hydrolyzed). Lipofectamine 2000, OptiMem®, MitoTracker, ERtracker, LysoTracker, pVAX1-lacZ plasmid, mMessage mMachine® T7 Ultra kit and Ambion MEGAclear™ kit from Life Technology.

Plasmid DNA preparation and GFP-mRNA production

pVAX-GFP (3697 bp) plasmid was obtained by modification of the commercial plasmid pVAX1-lacZ (6050 bp, Life Technology), by replacement of the β-galactosidase reporter gene by the enhanced Green Fluorescent Protein (eGFP, referred to as GFP thereafter) gene. The details of the construction are described elsewhere[16]. The plasmid contains the human cytomegalovirus (CMV) immediate-early promoter, a ColE1 type origin of replication and the kanamycin resistance gene for bacterial selection. Plasmid DNA (pDNA) was obtained by growing E.coli cultures (harbouring pVAX-GFP) overnight, in 2 L shake-flasks containing 250 mL LB medium and antibiotics (30 μg/mL of kanamycin). Then the plasmid were purified as described by means of EndoFree plasmid purification. The purified plasmid was diluted by Tris-EDTA (TE) buffer solution and stored at -20°C. The integrity of plasmid was confirmed by agarose gel electrophoresis. The purity and concentration of plasmid were determined by UV absorbance at 260 nm.
After linearizing the plasmid used as template, the mRNA was synthesized with mMessage mMachine® T7 Ultra kit from Ambion (Life Technology), in according with manufactured instructions. mRNA was purified by using the Ambion MEGAclear™ kit from Ambion (Life Technology). The integrity of mRNA was confirmed by agarose gel electrophoresis. The purity and concentration of mRNA were determined by UV absorbance at 260/280 nm, respectively.

PCL NPs and GFP-mRNA/PRM PCL NPs preparation

PCL nanoparticles were prepared by an emulsion-diffusion-evaporation method. Briefly, GFP-mRNA was reconstituted in RNase-free water and was complexed with a protamine sulphate solution by incubating at room temperature for 30 minutes on a rotary shaker. GFP-mRNA (20 μg/mL) was combined at various ratios, in particular 1:1, 1:3, 1:5, with the protamine sulphate (1 mg/mL) previously dissolved in NaCl 0.1 M. 100 mg amount of PCL was dissolved in 10 mL organic phase consisting of 9 mL ethyl acetate and 1 mL acetone for 1 hour under mild heating at 30°C. As for the aqueous phase, 100 mg PVA were stirred in 5 mL water for 2 hours at room temperature until a clear solution was obtained, after, GFP-mRNA/PRM complex solution was mixed. The organic phase was passed through a 0.22 μm syringe filter to remove any undissolved solids and subsequently added drop wise to the aqueous phase under constant stirring. The resulting microemulsion was kept under constant agitation on magnetic stirrer at 1000 rpm for 1 hour and was subsequently sonicated for 30 minutes. This colloidal preparation was diluted to a volume of 50 mL by adding water drop wise under stirring conditions (1000 rpm, magnetic stirrer), which resulted in nanoprecipitation. In order to remove the organic solvent and to harden the PCL nanoparticles, the suspension was treated with a rotary evaporator at 50 mbar at 40°C for 20 minutes. Next, the nanoparticle suspension was washed three time with RNase-free water by centrifugation at 12000 rpm for 10 minutes and then resuspended in water. The finished nanoparticle suspension was stored at 4°C for further use. To determine the concentration of nanoparticles (weight per volume), this suspension was centrifuged to 12000 rpm for 10 minutes; the supernatant was removed and the pellet was allowed to dry under a nitrogen stream before weighing. For preparing fluorescent PRM-FITC PCL nanoparticles, a 1 mg/mL PRM-FITC was added to PCL solution and the formulation was carried out as described earlier. The labeled nanoparticles were stored in the dark at 4°C until use.

Nanoparticles size, surface charge studies and stability

The average particle size and zeta potential of the prepared nanoparticles were determined by photon correlation spectroscopy using a Zetasizer Nano ZS90 (Malvern Instruments Ltd., USA) equipped with a 4.0mW He-Ne laser operating at 633 nm and an avalanche photodiode detector. Measurements were made at 25°C in aqueous solutions (pH 7). The PCL NPs solution (1 mg/mL) was passed through a 0.45 μm pore size filter before measurements and appropriately diluted if necessary according to the instrument's requirements. The stability of mRNA/PRM PCL NPs was tested under physiological conditions. Briefly, nanoparticles were incubated in complete DMEM medium at 37°C, and the size variation was measured over a period of 8 days by Dynamic Light Scattering (DLS) analysis. Representative measurements of three distinct sets of data have been reported (*Student t- test, $P < 0.05$*).

Scanning Electron Microscopy (SEM) and Atomic Force Microscopy (AFM)

For SEM analysis (RHAIT 150), samples were prepared by applying a drop of the particle suspension to a SiO2 wafer and then drying overnight. Prior to SEM observation, the samples were sputter-coated with a 10 nm gold layer to make them electronically conductive and to avoid electronic charging during SEM imaging. The morphological characterization has been performed by tapping mode AFM using a Solver PRO Scanning Probe Microscope (NT-MDT) in air at room temperature, we used TESPA (Veeco, USA) silicon cantilevers of 20-80 N/m spring constant and resonance frequency of around 300 kHz. A drop of sample suspension was applied to a silicon support and then drying overnight.

Encapsulation efficiency and *in vitro* mRNA release study

The encapsulation efficiency of the nanoparticles was determined by analysing the supernatant of the final emulsion, once the nanoparticles was removed from it, by centrifugation

at 12000 rpm for 10 minutes. For the estimation of mRNA present in the supernatant, absorbance was measured in a spectrophotometer at 260 nm. The amount of mRNA encapsulated and the percent encapsulation in the nanoparticles is given by following equations:

mRNA encapsulated = total mRNA – filtrate mRNA

% Encapsulation =(Encapsulated mRNA)/(Total mRNA) x 100

The release of mRNA from PCL nanoparticles was measured in TE buffer. Briefly, a known amount of lyophilized GFP mRNA/PRM PCL nanoparticles (50 mg) were dispersed in 5 mL of phosphate buffer 1x (PBS) pH 7.4 and 500 µl of sample was dialyzed in a large volume of PBS 1x pH 7.4 and pH 5.0, and maintained at 37°C ± 0.5°C under stirring at 50 rpm. At specified time intervals, the samples were centrifuged (12000 rpm for 10 minutes) and supernatants were collected. Samples were taken and analysed in triplicates. The concentration of GFP mRNA was determined from the corresponding absorbance measured in spectrophotometer at 260 nm. Representative measurements of three distinct sets of data have been reported (*Student t- test, $P < 0.05$*).

Gel Retardation assay

The electrophoretic mobility of the prepared complexes and nanoparticles with different weight ratio of PRM/GFP-mRNA, (ratio 1:1, 1:3 and ratio 1:5) was determined by 1% agarose gel in TBE 1x (Tris/borate/EDTA) buffer with 0.5 µg/mL of ethidium bromide at 110 V for 30 min. The gel was visualized under a UV transilluminator.

Cell culture

Human osteosarcoma cells (MG63), human cervix carcinoma cells (HeLa) and mouse embryonic fibroblast cells (NIH 3T3) were maintained in DMEM supplemented with 10% FBS, 100 U/mL penicillin, 100 mg/mL streptomycin, 5% L-glutamine and 5% sodium pyruvate, in a humidified incubator at 37°C, 5% CO2, and 95% relative humidity. Upon reaching confluence, cells were passaged using 0.25% trypsin-EDTA. Cells at passages 3-10 were used in the following experimental assays.

Cytotoxicity assay

Cytotoxicity viability was evaluated by 3-[4,5-dimethylthiazol-2-yl]-2,5-diphenyl tetrazolium bromide (MTT) assay against mouse embryonic fibroblast cells (NIH 3T3), human cervix carcinoma cells (HeLa) and human osteosarcoma cells (MG63) incubated with PCL nanoparticles (1 mg/mL). Cells were seeded on 24-well plates at a density of 10^5 cells/well in complete culture media. After 24 h, the media without FBS were used to replace the usual ones, and PCL nanoparticles were resuspended in complete medium and were added each well. Untreated samples were used as the control groups. After an appropriate incubation period, the cultures were removed from the incubator and the MTT solution added in an amount equal to 10% of the culture volume. Then the cultures were returned to incubator and incubated for 3 hours. After the incubation period, the cultures were removed from the incubator and the resulting MTT formazan crystals were dissolved with acidified isopropanol solution to an equal culture volume. The plates were read within 1 hour after adding acidified isopropanol solution. The absorbance was spectrophotometrically measured at wavelength 570 nm and the background absorbance measured at 690 nm substracted. The percentage viability is expressed as the relative growth rate (RGR) by equation:

RGR= (D_sample/D_control)x 100%

where Dsample and Dcontrol are the absorbances of the sample and the negative control. Representative measurements of three distinct sets of data have been reported (*Student t- test, $P < 0.05$*).

Intracellular localization study

To determine the cellular uptake of the PRM-FITC PCL NPs we seeded 10^5 cells/mL in sterile glass-culture slide. The cells were incubated with the PRM-FITC PCL NPs dispersions at a concentration of 0.05 mg/mL. After 3 hours of incubation at 37°C, the culture medium was removed, and the cells were washed three times with phosphate buffered saline. For fluorescent microscopic observation, cells were fixed in situ for 5 minutes in 3.7% formaldehyde and mounting with fluoroshield with DAPI. To study the intracellular localization of PRM-FITC PCL NPs immunostaining with LysoTracker Red (Life technology), MitoTracker Red (Life technology) and ER-Tracker Red (Life technology) were performed, in according with manufactur's instructions, to label lysosomes, mitocrondria and endoplasmic reticulum, respectively. Confocal micrographs were taken with Leica confocal scanning system mounted into a Leica TCS SP5 (Leica Microsystem GmbH, Mannheim, Germany), equipped with a 63 X oil immersion objective and spatial resolution of approximately 200 nm in x-y and 100 nm in z. The 3D confocal scanning is performed by reconstructing the photoluminescence coming from different focalized slices with a sequential image acquisition. The optical sections were collected in transverse x-z and y-z planes.

GFP mRNA/PRM PCL nanoparticles transfection and GFP detection

For *in vitro* transfection study, the mouse embryonic fibroblast cells (NIH 3T3), human cervix carcinoma cells (HeLa) and human osteosarcoma cells (MG63) were split one day prior to transfection and plated at a density of 10^5 cells. Before transfection, the culture medium was replaced with OptiMem. The cells were transfected with mRNA/PRM PCL NPs containing 1 µg of GFP mRNA at 37°C for 4 hours. Then the GFP mRNA/PRM PCL NPs were removed and the cells were incubated in fresh DMEM with 10% FBS at 37°C, 5% CO2, and 95% relative humidity for another 24 hours. GFP mRNA and Lipofectamine 2000 (Life technology) complexes were used as positive control of mRNA efficacy, according to manufacturer's instruction. For fluorescent microscopic observation, cells were fixed in situ for 5 minutes in 3.7% formaldehyde and mounting with fluoroshield with DAPI. Confocal micrographs were taken with Leica confocal scanning system mounted into a Leica TCS SP5 (Leica Microsystem GmbH, Mannheim, Germany), equipped with a 63 X oil immersion objective and spatial resolution of approximately 200 nm in x-y and 100 nm in z.

Quantitative measure of transfection with GFP mRNA/PRM PCL NPs or Lipofectamine 2000, the cells were lysate by 50 mL 0.1% Triton X-100 in 0.2 M NaOH. Cell-associated GFP fluorescence were quantified by analysing the cell lysates in a fluorescence plate reader (λ excitation 488 nm, λ emission 508 nm). The quantity of GFP was expressed as the percentage of the fluorescence associated with cells *vs* that present in the not-transfected cells. Representative measurements of three distinct sets of data have been reported (*Student t- test, $P < 0.05$*).

Results and Discussion

Messenger RNA has a high potential to produce proteins or peptides for therapeutic purposes in a safe manner without any risk of random integration into the genome. Although pioneering studies to transfect mRNA into cells using a non-viral method, the interest in the clinical use of mRNA has been limited for a long time. There are two major problems associated with mRNA introduction: mRNA is considered to be unstable to obtain sufficient protein expression in clinical settings[17] and mRNA induces strong immune reactions through recognition by Toll-like receptors (TLRs)[18,19], hampering repeated mRNA administration. Thus, the requirement of an effective mRNA non-viral delivery system to overcome the instability of mRNA should be further explored to realise *in vivo* mRNA administration. Although some strategies have been reported for non-viral *in vivo* mRNA administration, including injection of naked mRNA[20] in combination with physical pressure such as electroporation or gene gun[21] and the usage of synthetic carriers based on cationic lipids and polymers[22,23], low efficiency and short duration of protein expression remain significant problems to be solved. These issues motivated us to apply a new methodology using our non-viral polymeric carrier for in vitro mRNA administration.

Synthesis and characterization of PCL nanoparticles loaded with GFP mRNA

The GFP mRNA loaded PCL nanoparticles prepared by an adapted emulsion-diffusion-solvent evaporation method as shown in **Scheme 1**. GFP mRNA-protamine complexes were formed in aqueous solution with the objective of enhancing the loading of the mRNA molecules, for this aim we have performed a partial neutralization of the mRNA molecules with the positively charged protamine. Then GFP mRNA-PRM complexes were mixed with a aqueous solution of PVA and this aqueous core (water phase) was coated with the oil phase containing the PCL molecules.

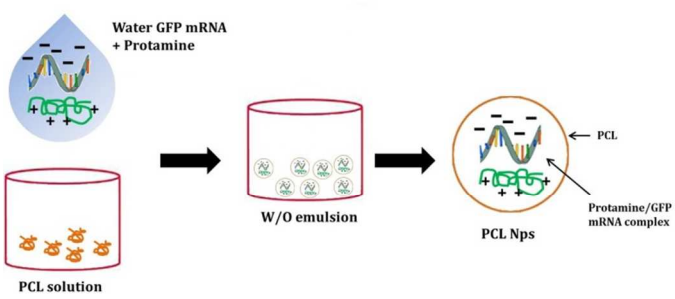

Scheme 1. Schematic illustration of the fabrication process of PCL nanoparticles incorporating GFP-mRNA/Protamine complexes. A emulsion-diffusion-evaporation method is used for the synthesis of the nanostructures. W and O represent the water phase and oil phase, respectively.

The synthesis protocol was optimized to obtain non-aggregating, spherical in shape with smooth surface NPs as shown the AFM and SEM images (**Fig. 1A** and **1C**, respectively). The nanoparticles observed by AFM and SEM have a spherical geometry with a good size distribution. The surface of these nanoparticles as observed under SEM was free from any pores or cracks and reasonably monodisperse nanoparticles form by polymers, all exhibiting a smooth surface morphology (**Fig. 1C**). The resulting NPs were characterized for their physicochemical properties, as size and surface zeta potential. As shown in **Fig. 1D**, PCL nanoparticles had a zeta potential of -4.72 mV ± 0.402 mV and an average diameter of 247.43 nm ± 0.577 nm (**Fig. 1E** and **1B**) with a polydispersion index (PdI) of 0.334 ± 0.040. The negative charge of mRNA loaded PCL NPs confirms that the mRNA-PRM complexes were engulfed in the PCL NPs hydrophilic core and fully covered by the PCL and PVA composite shell.

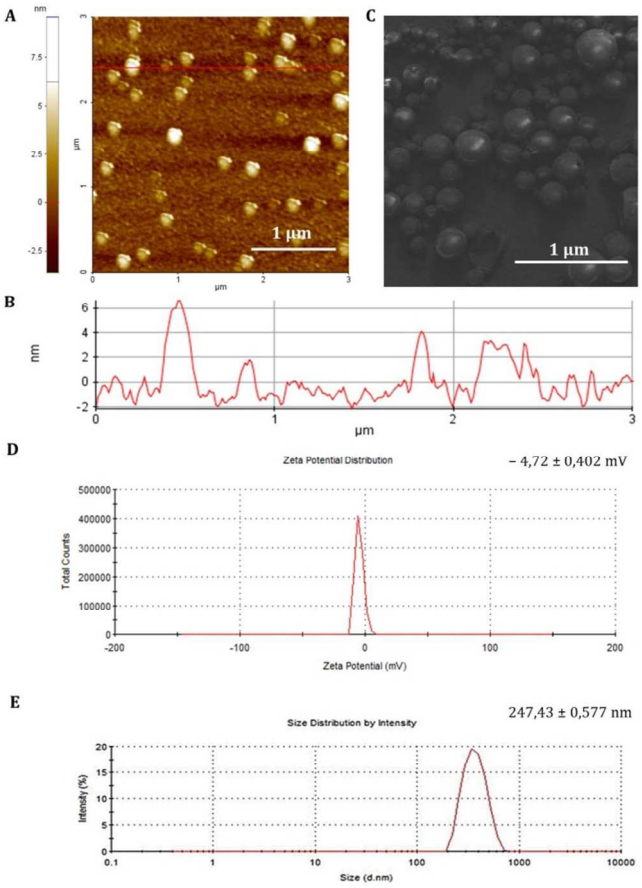

Fig. 1. Physicochemical characterization of GFP-mRNA-loaded PCL Nps. (A) AFM image of dried PCL Nps (B) red line profile of AFM image. (C) SEM image showing the size and morphology of dried sample. *Scale bars:* 1 µm (D) Surface zeta potential distribution demonstrating the uniformity of the sample population. Mean ± standard deviation is presented in the upper corner of the panel. (E) Size distribution from DLS analysis showing the mean ± standard deviation of PCL Nps. Values represents the mean ± standard deviation of four independent experiments.

The stability of the mRNA loaded NPs was tested under physiological conditions. NPs were incubated in complete DMEM medium at 37°C, and the size variation was measured over a period of 8 days by DLS analysis. As shown in **Fig. 2A**, over a period of 8 days PCL NPs maintain their hydrodynamic size of about 247 nm, demonstrating no significant aggregation. In addition, no significant change in PdI was observed, supporting evidence of particle stability in physiological conditions.

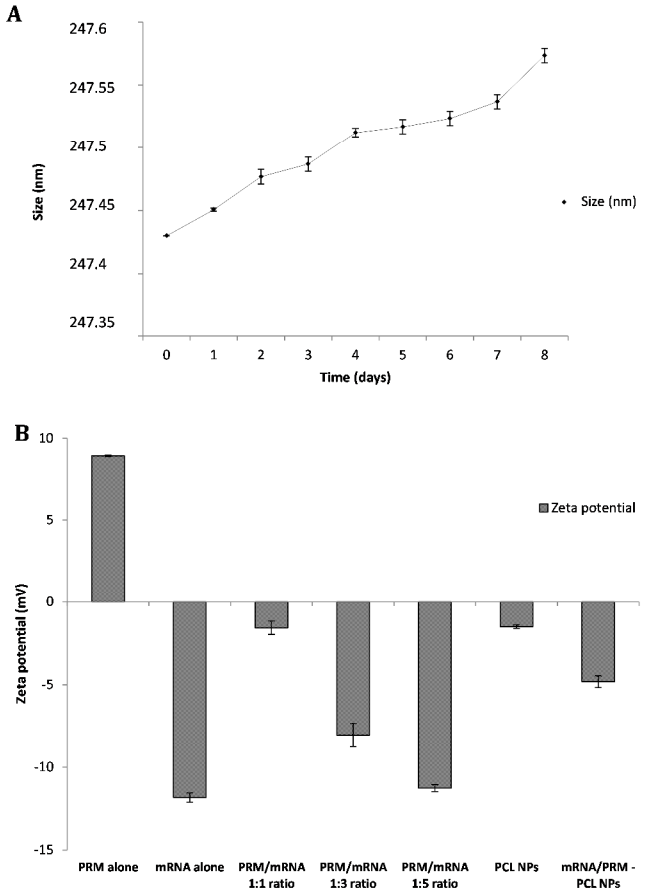

Fig. 2. (A) Size distribution from DLS analysis showing the effect of the incubation of PCL NPs in complete DMEM medium at 37°C on the stability of the NPs. Size distribution of the NPs are determined by DLS analysis performed each time point. (B) Zeta potential of the PRM alone, mRNA alone, mRNA-PRM complexes at different ratio (PRM:mRNA, in particular 1:1, 1:3 and 1:5), PCL nanoparticles and mRNA/PRM complexes loaded in PCL NPs. The ratio PRM:mRNA 1:1 was chosen for NPs synthesis. Representative measurements of three distinct sets of data have been reported (*t-Student* test, $P < 0.05$).

GFP mRNA/PRM loading in PCL NPs and mRNA release kinetics under different physiological conditions

The materials used in the preparation of the mRNA loaded PCL NPs are mostly negatively charged, except the positively charged protamine. The PCL and mRNA show a negative zeta potential (see **Fig. 2B**). Therefore to form stabile NPs, the mRNA molecules were partially neutralized by forming complexes with protamine. This is a cationic polyelectrolyte, which can efficiently form stable complexes with the negatively charged mRNA. As shown in **Fig. 2B**, protamine and mRNA were mixed at different ratios. By increasing the PRM:mRNA ratio from 1:1 to 1:5, the zeta potential of the complex was modulated. An PRM:mRNA ratio of 1:1 was chosen for the synthesis of the mRNA loaded PCL NPs. In addition, the binding capacity of cationic protamine and subsequent of PCL NPs for mRNA was investigated by assessing the complexes' electrophoretic mobility in an agarose gel. As shown in **Fig. 3**, agarose gel electrophoresis retardation assay was performed with different weight ratio of PRM/GFP-mRNA, ratio 1:1, 1:3 and ratio 1:5. If a mRNA-PRM complex or mRNA/PRM-PCL NPs were formed efficiently, that is, all mRNA is bound to the nanoparticles, no band for free mRNA can be observed, and the immobile complex remains in the starting zone of the gel.

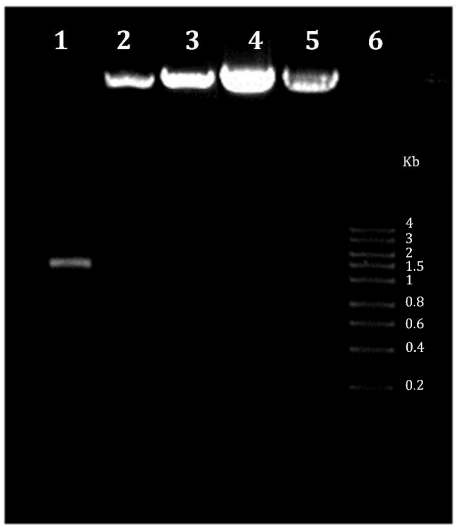

Fig. 3. Agarose gel electrophoresis retardation assay. Lane 1: mRNA GFP free; Lane 2: PRM/GFP-mRNA ratio 1:1; Lane 3: PRM/GFP-mRNA ratio 1:3; Lane 4: PRM/GFP-mRNA ratio 1:5; Lane 5: PRM/GFP-mRNA loaded in PCL NPs; Lane 6: RNA marker.

The encapsulation efficiency of the PCL NPs was found to be 58.47 ± 0.65% and the release of mRNA molecules from the PCL NPs was studied over time at two different pH (7.4 and 5.0) that were selected to mimic the physiological conditions that NPs would found in the circulation (pH 7.4) and in the acidic environment of the cell endosomes (pH 5.0), respectively. The percentage of mRNA released over time is shown in **Fig 4**. For a circulating PCL NPs (pH 7.4), the release rate is extremely low within the first few hours and after 48 hours, only about 25% of the loaded mRNA is released. On the contrary, within a cell endosome (pH 5.0), about 60% of the mRNA molecules are released within the same time window post incubation. These different release kinetics are indeed associated to different release mechanisms. At pH 7.4, the mRNA release is mostly governed by the diffusion of the molecules out of the NP hydrophilic core, through the pores of the PCL/PVA shell, and eventually in the surrounding environment, thus confirming that in neutral pH the mRNA release is mostly driven by passive diffusion through the pores of the polymeric shell. On the contrary, the rapid release observed at pH 5.0 is most likely associated with the hydrolysis of the PCL/PVA shell under acid conditions that would progressively increase the nanoparticles porosity with consequent rapid release of its payload.

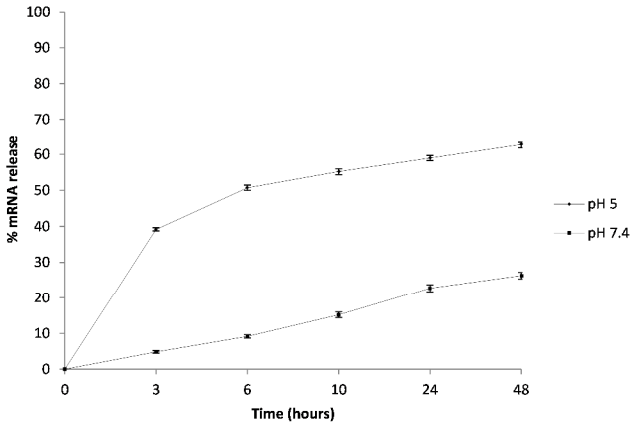

Fig. 4. *In vitro* cumulative percent of release of GFP mRNA from PCL nanoparticles over time. Measurements were performed at 37°C and a pH 5.0 or pH 7.4. Representative measurements of three distinct sets of data have been reported (t-Student test, $P < 0.05$).

Cytotoxicity of PCL nanoparticles and intracellular localization

In vitro cytotoxicity of the PCL nanoparticles was estimated by performing a MTT test on mouse embryonic fibroblast cells (NIH 3T3), human cervix carcinoma cells (HeLa) and human osteosarcoma cells (MG63). In particular, it was important to assess cytotoxicity of the nanoparticles upon 24 hours of incubation since the cells would be in an exponential growth phase during this period and any toxicity that reflects inhibition of proliferation and/or cell death would be clearly visible[24].
As shown in **Supplementary Fig. S1**, the PCL NPs did not show any significant effect on the cell viability for time frames that we have tested.
To identify the intracellular distribution of PRM-FITC PCL nanoparticles (green channel in CLSM images of **Supplementary Fig. S2, S3 and S4**), we performed co-localization assays on NIH 3T3 fibroblasts, HeLa cells and MG63 osteoblasts with MitoTracker, ERtracker and Lysotracker markers (red channel in CLSM images of **Supplementary Fig. S2, S3 and S4**) for mitochondria, endoplasmic reticulum and lysosomes, respectively. As shown in Supplementary Figures S2, S3 and S4 high co-localization (yellow present in the merge channel of CLSM images of **Supplementary Fig. S2, S3 and S4**) of green fluorescence PRM-FITC PCL nanoparticles and red fluorescence of MitoTracker marker was observed. and its released mRNA were primarily transported to mitochondria. Conversely, low co-localization signal with red fluorescent of ERtracker and Lysotracker, were observed, and this indicates that the mRNA is not typically localized within endoplasmic reticulum and lysosomes. Thanks to the presence of protamine it's possible overcame the mRNA degradation inside the lysosomes/endosomes and more mRNA following escape from endosomes resulting in high expression efficiency. The positively charged arginine groups of protamine could bind to the acidic phospholipid groups in the membrane of the lysosomes and induced lysosomal leakage *in vitro*[25]. The polycationic protamine-coated nanoparticles might exert sufficient buffering capacity in lysosomes to facilitate lysosomal escape[26-27], which resulted in cytoplasm release of exogenous molecules.

In vitro transfection efficiency

PCL NPs loaded with GFP mRNA/PRM were incubated with NIH 3T3 fibroblasts, HeLa cells and MG63 osteoblasts for 4 hours. After 24 hours post transfection, cells were fixed, and their nuclei were stained with DAPI. As shown in **Fig. 5**, lateral, front, and top views show the fluorescent GFP molecules expressed by the transfected mRNA accumulating within the cell and localizing either cytoplasm and perinuclear regions.

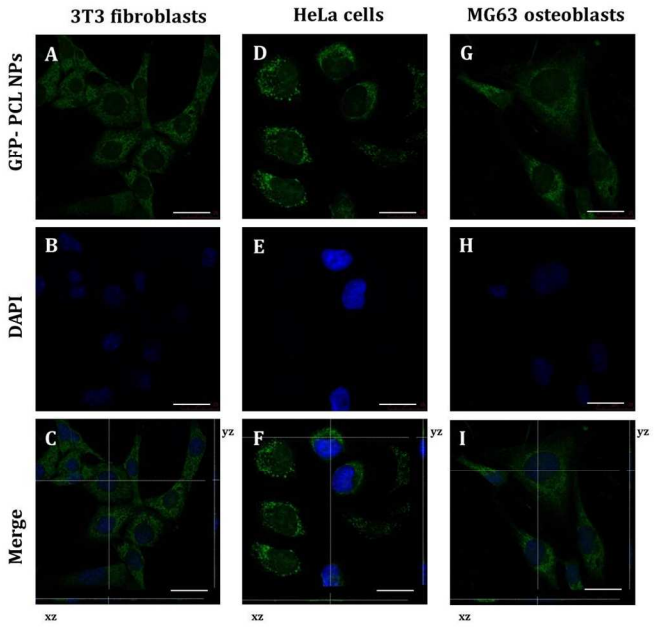

Fig. 5. CLSM images of GFP-mRNA expression delivered by PCL NPs of the transfected NIH 3T3 fibroblasts(A,B,C), HeLa cells (D,E,F) and MG63 osteoblasts (G,H,I) after 24 hours of incubation. CLSM images A,D,G shown the expression of GFP (green). Cell nuclei were counterstained with DAPI (blue) as shown in the CLSM images B,E,H. Each merge of confocal images (C,F,I) reports the corresponding Z-stack optical sections (yz and xz) obtained through photoluminescence reconstruction in the z-direction, with a z-resolution of 200 nm to confirm the spatial GFP expression inside cells. *Scale bars: 25 μm.*

To better characterize the PCL NPs contribution to the intracellular delivery of mRNA molecules, the internalization efficiency of different systems were compared, namely, GFP mRNA-PCL NPs and GFP mRNA-lipofectamine. In particular, Lipofectamine 2000 is a cationic liposome formulation that functions by complexing with nucleic acid molecules, allowing them to overcome the electrostatic repulsion of the cell membrane and to be taken up by the cell.[28] The resulting CLSM images are shown in **Fig. 6.**

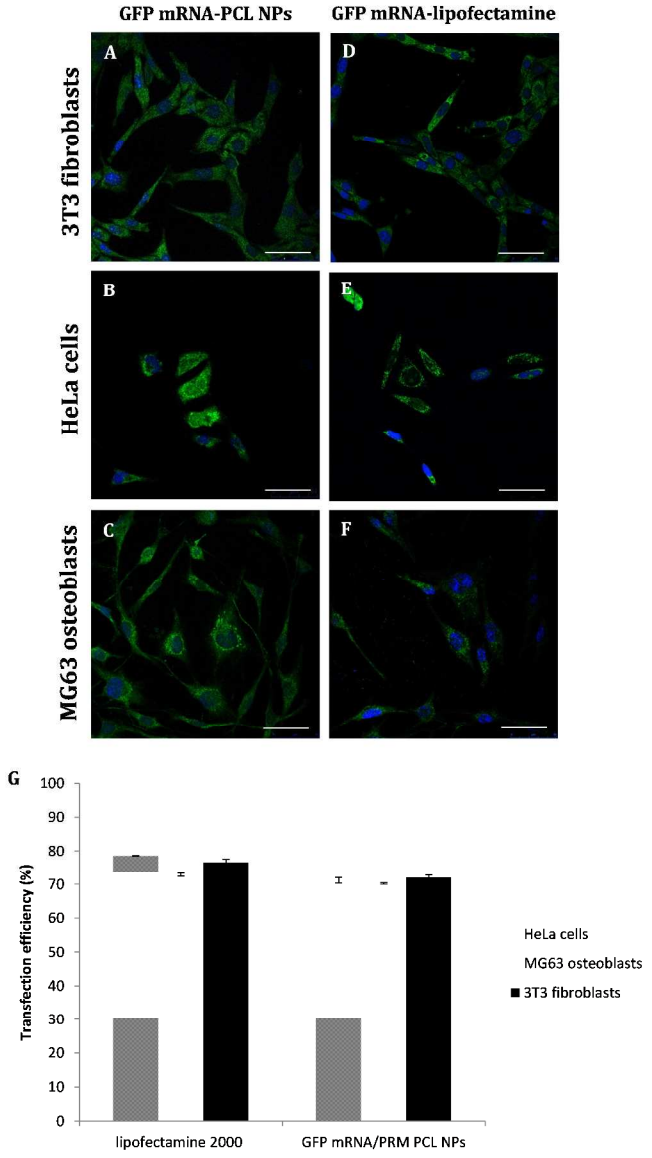

Fig. 6. CLSM images of differential GFP-mRNA expression (green) delivered by PCL NPs (A,B,C) and Lipofectamine 2000 (C,D,E) of the transfected NIH 3T3 fibroblasts (A,D), HeLa cells (B,E) and MG63 osteoblasts (C,F) after 24 hours of incubation. Cell nuclei were counterstained with DAPI (blue). *Scale bars: 50 μm*. (G) Transfection efficiency (%) of mRNA-GFP delivery by PCL NPs or Lipofectamine 2000. Representative measurements of three distinct sets of data have been reported *(t-Student test, $P < 0.05$)*.

As expected, the commercially available system designed for *in vitro* cell transfection, GFP mRNA-lipofectamine delivered the mRNA molecules with high efficiency, as demonstrated by the several green fluorescent due to the expression of GFP accumulating within the cells. Notably, the GFP mRNA-PCL NPs and GFP mRNA-lipofectamine complexes presented comparable delivering efficiency, demonstrating the high transfection efficiency of our NPs, as evident in the **Fig. 6G**. It's evident from the CLSM images that our PCL NPs mediated transfection efficiency is substantially higher as seen by the number of cells expressing GFP as a result of translation of mRNA as compared to transfection efficiency obtained with lipofectamine, used as positive control. This finding confirms the functional integrity of the mRNA during its encapsulation and subsequent release from the nanoparticles.

Conclusions

Transcript replacement therapy using non-viral vectors could be a promising approach for the treatment of inherited genetic disorders for which other treatment options are limited or unavailable. Moreover, administration of mRNA may have potential in the field of regenerative medicine and for the treatment of degenerative diseases. A new method to improve the transfection efficiency of GFP mRNA, used as example, loaded in PCL NPs as non-viral vectors is discussed in this work. Our non-viral system present a characteristic core-shell architecture based on the assembly of mRNA molecules and protamine complex and PCL. The PCL NPs has a strong potential to function as an effective mRNA-containing carrier with high stability and stealth properties, thereby addressing the issue of mRNA instability. In the future, the retention and release kinetics of mRNA inside the nanoparticles should be highly controlled by the molecular design of the nanoparticles. In this manner, we believe that even more prolonged expression from mRNA will be achieved using the PCL nanoparticles system to fulfil the various needs of treatments and administration routes, opening the door to various new therapeutic strategies using mRNA.

Acknowledgements
This study was supported by MAAT - Nanotecnologie molecolari per la salute dell'uomo e l'ambiente (PON R&C 2007-2013, project's code PON02_00563_3316357). No writing assistance was utilized in the production of this manuscript. The authors have no competing interests to disclose.

Notes and references

[a]National Nanotechnology Laboratory, Institute Nanoscience CNR (NNL, CNR-NANO) via Arnesano, Lecce, Italy;
[b]Dept. Matematica e Fisica 'Ennio De Giorgi', University of Salento, via Monteroni, Lecce, Italy;
[c]Italian Institute of Technology (IIT) - Center for Biomolecular Nanotechnologies, via Barsanti, Arnesano, Italy
*Corresponding author contact - Mail: ilariaelena.palama@nano.cnr.it

1 V.F. Van Tendeloo, ,P. Ponsaerts, Z.N. Berneman, *Curr Opin Mol Ther*, 2007, **9**, 423.
2 R.M. Steinman, H. Hemmi, *Curr Top Microbiol Immunol*, 2006, **311**, 17.
3 L. Warren, P.D. Manos, T. Ahfeldt, Y.H. Loh, H., Li, F. Lau, *Cell Stem Cell*, 2010, **7**, 618.
4 H. Wurtele, K.C. Little, P. Chartrand, *Gene Therapy,* 2003, **10**, 1791.
5 B. Probst, B. Weide, B.J. Scheel, I. Pichler, H.G. Hoerr, S. Rammensee, S. Pascolo, *Gene Therapy*, 2007, **14**, 1175.
6 Z. Amoozgar, J. Park, Q. Lin, Y. Yeo, *Mol. Pharmaceutics*, 2012, **9**, 1262.
7 I.S. Kim, S.K. Lee, Y.M. Park, Y.B. Lee, S.C. Shin, K.C. Lee, I.J. Oh, *Int. J. Pharmaceutics,* 2005, **298**, 255.
8 I.E. Palamà, M. Musarò, A.M.L. Coluccia, S. D'Amone, G. Gigli, *Journal of Drug Delivery*, 2011, **1**.

9 I.E. Palamà, A.M.L. Coluccia, G. Gigli, *Nanomedicine*, 2013, doi: 10.2217/NNM.13.147.
10 A. Alshamsan, A. Haddadi, S. Hamdy, J. Samuel, A.O. El-Kadi, H. Uludag, A. Lavasanifar, *Mol. Pharmaceutics*, 2010, **5**, 1643.
11 K.A. Woodrow, Y. Cu, C.J. Booth, J.K. Saucier-Sawyer, M.J. Wood, W.M. Saltzman, *Nat. Mater.*, 2009, 8, 526.
12 M.D. Bhavsar, M.M. Amiji, Development of Novel Biodegradable Polymeric Nanoparticles-in-Microsphere Formulation for Local Plasmid DNA Delivery in the Gastrointestinal Tract, AAPS Pharm Sci Tech, 9 (1) (2008) 288-294.
13 I.E. Palamà, A.M.L. Coluccia, A. Della Torre, V. Vergaro, E. Perrone, R. Cingolani, R. Rinaldi, S. Leporatti, *Science of Advanced Materials*, 2010, **2**, 1.
14 I.E. Palamà, S. Leporatti, E. De Luca, C. Gambacorti-Passerini, N. Di Renzo, M. Maffia, R. Rinaldi, G. Gigli, R. Cingolani, A. M.L. Coluccia, *Nanomedicine*, 2010, **5**, 419.
15 F.L. Sorgi, S. Bhattacharya, L. Huang, *Gene Ther*, 1997, **4**, 961.
16 A.R. Azzoni, S.C. Ribeiro, G.A. Monteiro, and D.M. F. Prazeres, *Journal of Gene Medicine*, 2007, **9**, 392.
17 G. Tavernier, O. Andries, J. Demeester, N.N Sanders, S.C. De Smedt, *et al., J Control Release*, 2011, **150**, 238.
18 F. Heil, H. Hemmi, H. Hochrein, F. Ampenberger, C. Kirschning, *et al*., *Science*, 2004, **303**, 1526.
19 K. Kariko, H. Ni, J. Capodici, M. Lamphier, D. Weissman, *J Biol Chem*, 2004, **279**, 12542.
20 J. Probst, B. Weide, B. Scheel, B.J. Pichler, I. Hoerr, *et al*., *Gene Ther*, 2007, **14**, 1175.
21 P. Qiu, P. Ziegelhoffer, J. Sun, N.S. Yang, *Gene Ther*, 1996, **3**, 262.
22 S. Zou, K. Scarfo, M.H. Nantz, J.G. Hecker*, Int J Pharm,* 2010, **389**, 232.
23 X. Su, J. Fricke, D.G. Kavanagh, D.J. Irvine, *Mol Pharm*, 2011, **8**, 774.
24 N. Nafee, M. Schneider, U.F. Schaefer, C.M. Lehr, *International Journal of Pharmaceutics*, 2009, **381**, 130.
25 E.V. Rukavishnikova, T.A. Korolenko, T. Sassa, T.Oka, S. Horiuchi, Y. Natori, *FEBS Lett*, 1995, **369**, 217.
26 T. Storni, T.M. Kündig, G. Senti, P. Johansen, *Adv Drug Deliv Rev*, 2005, **57**, 333.
27 S. Fischer, E. Uetz-von Allmen, Y. Waeckerle-Men, M. Groettrup, H.P. Merkle, B. Gander, *Biomaterials*, 2007, **28**, 994.
28 B. Dalby, S. Cates, A. Harris, E.C. Ohki, M.L. Tilkins, P.J. Price, V.C. Ciccarone, *Methods*, 2004, **33**, 95.

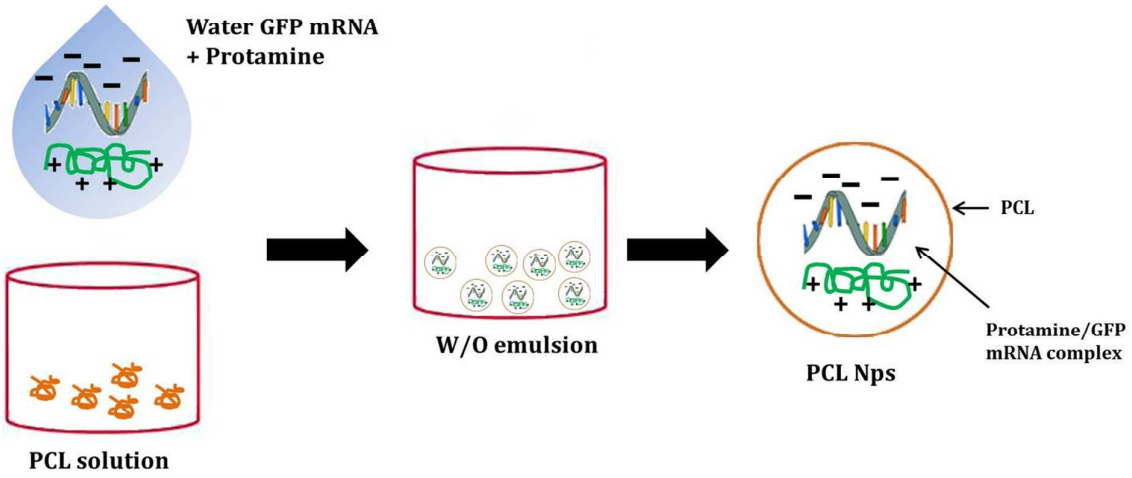

Scheme 1. Schematic illustration of the fabrication process of PCL nanoparticles incorporating GFP-mRNA/Protamine complexes. A emulsion-diffusion-evaporation method is used for the synthesis of the nanostructures. W and O represent the water phase and oil phase, respectively.

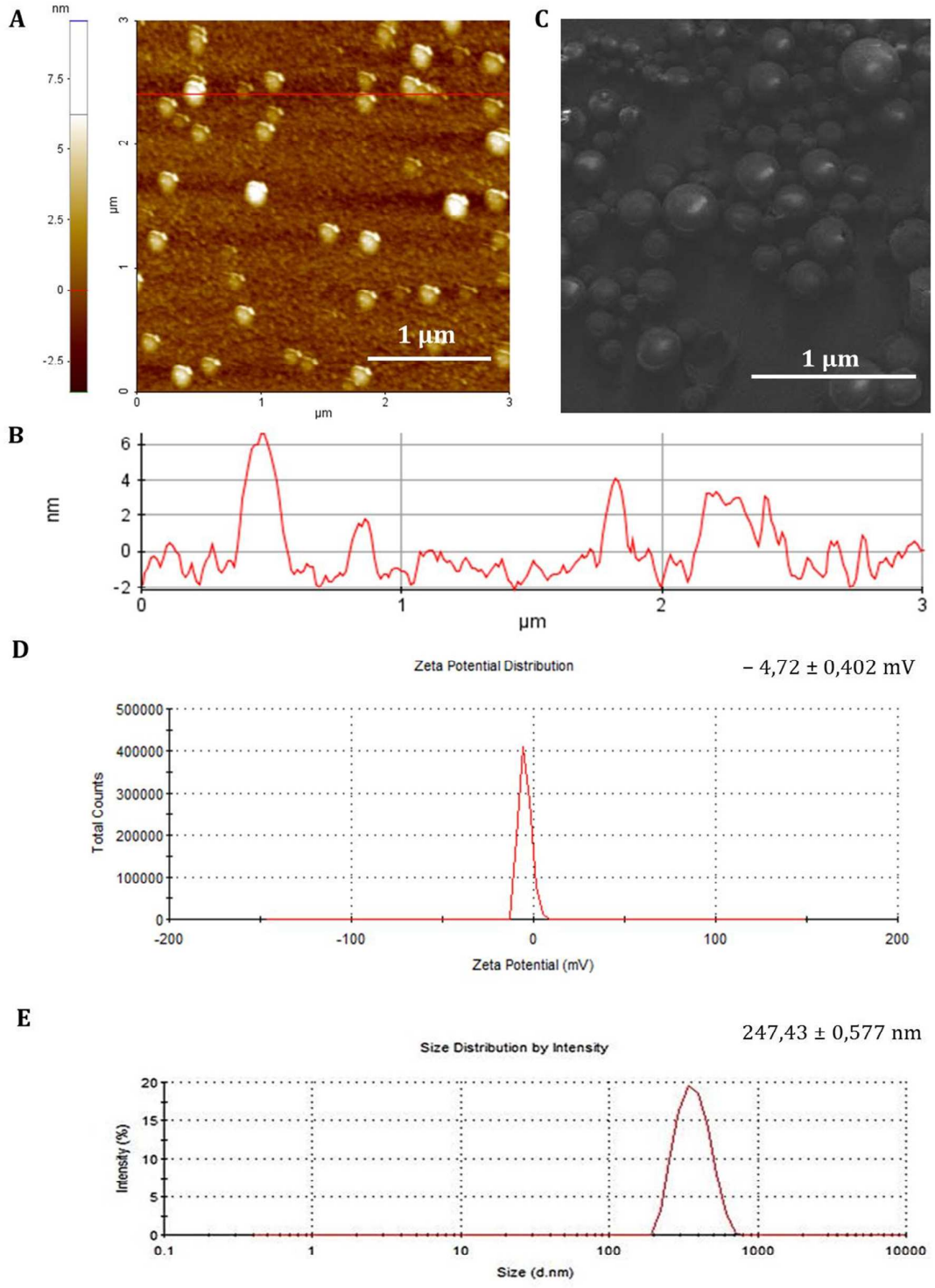

Fig. 1. Physicochemical characterization of GFP-mRNA-loaded PCL Nps. (A) AFM image of dried PCL Nps (B) red line profile of AFM image. (C) SEM image showing the size and morphology of dried sample. *Scale bars:* 1 µm (D) Surface zeta potential distribution demonstrating the uniformity of the sample population. Mean ± standard deviation is presented in the upper corner of the panel. (E) Size distribution from DLS analysis showing the mean ± standard deviation of PCL Nps. Values represents the mean ± standard deviation of four independent experiments.

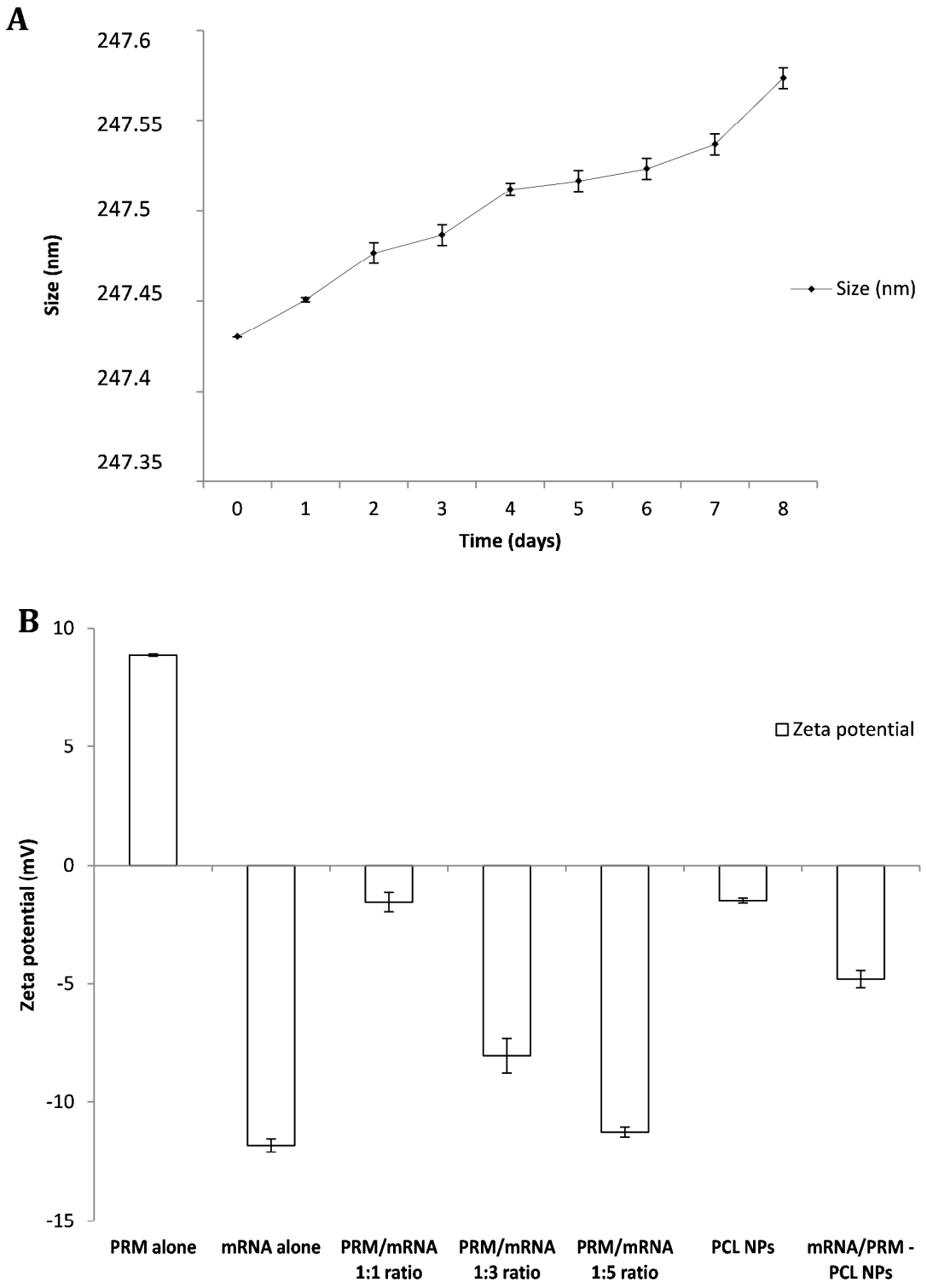

Fig. 2. (A) Size distribution from DLS analysis showing the effect of the incubation of PCL NPs in complete DMEM medium at 37°C on the stability of the NPs. Size distribution of the NPs are determined by DLS analysis performed each time point. (B) Zeta potential of the PRM alone, mRNA alone, mRNA-PRM complexes at different ratio (PRM:mRNA, in particular 1:1, 1:3 and 1:5), PCL nanoparticles and mRNA/PRM complexes loaded in PCL NPs. The ratio PRM:mRNA 1:1 was chosen for NPs synthesis. Representative measurements of three distinct sets of data have been reported (*t-Student test, $P < 0.05$*).

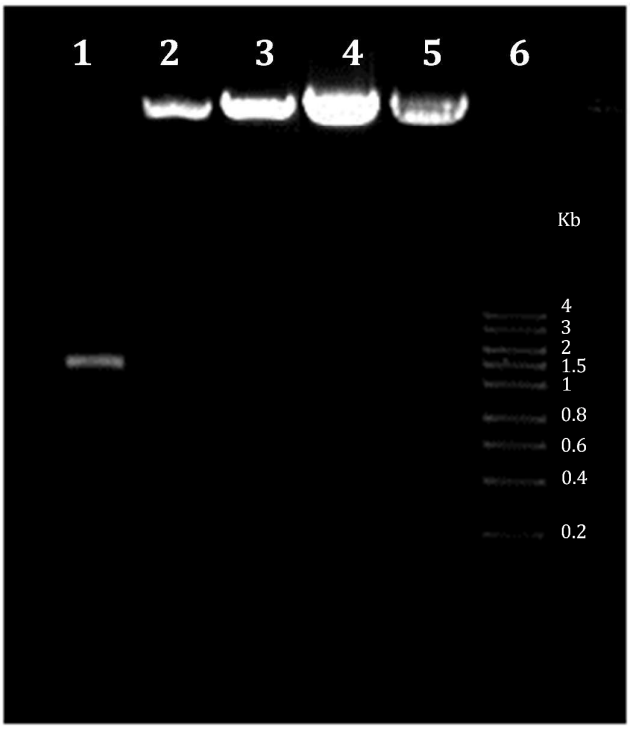

Fig. 3. Agarose gel electrophoresis retardation assay. Lane 1: mRNA GFP free; Lane 2: PRM/GFP-mRNA ratio 1:1; Lane 3: PRM/GFP-mRNA ratio 1:3; Lane 4: PRM/GFP-mRNA ratio 1:5; Lane 5: PRM/GFP-mRNA loaded in PCL NPs; Lane 6: RNA marker.

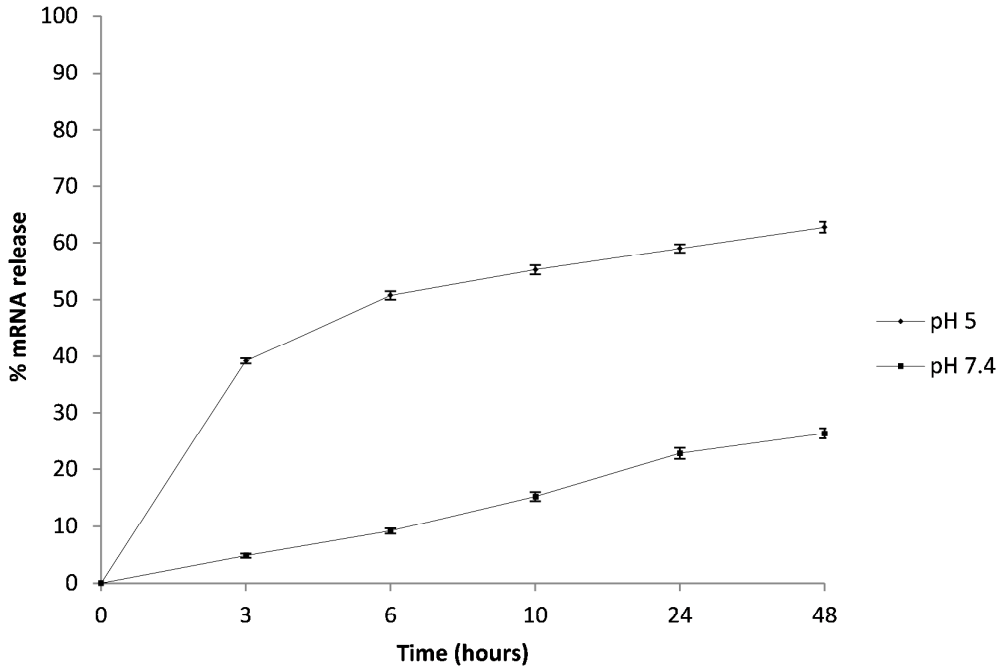

Fig. 4. *In vitro* cumulative percent of release of GFP mRNA from PCL nanoparticles over time. Measurements were performed at 37°C and a pH 5.0 or pH 7.4. Representative measurements of three distinct sets of data have been reported (*t-Student test, $P < 0.05$*).

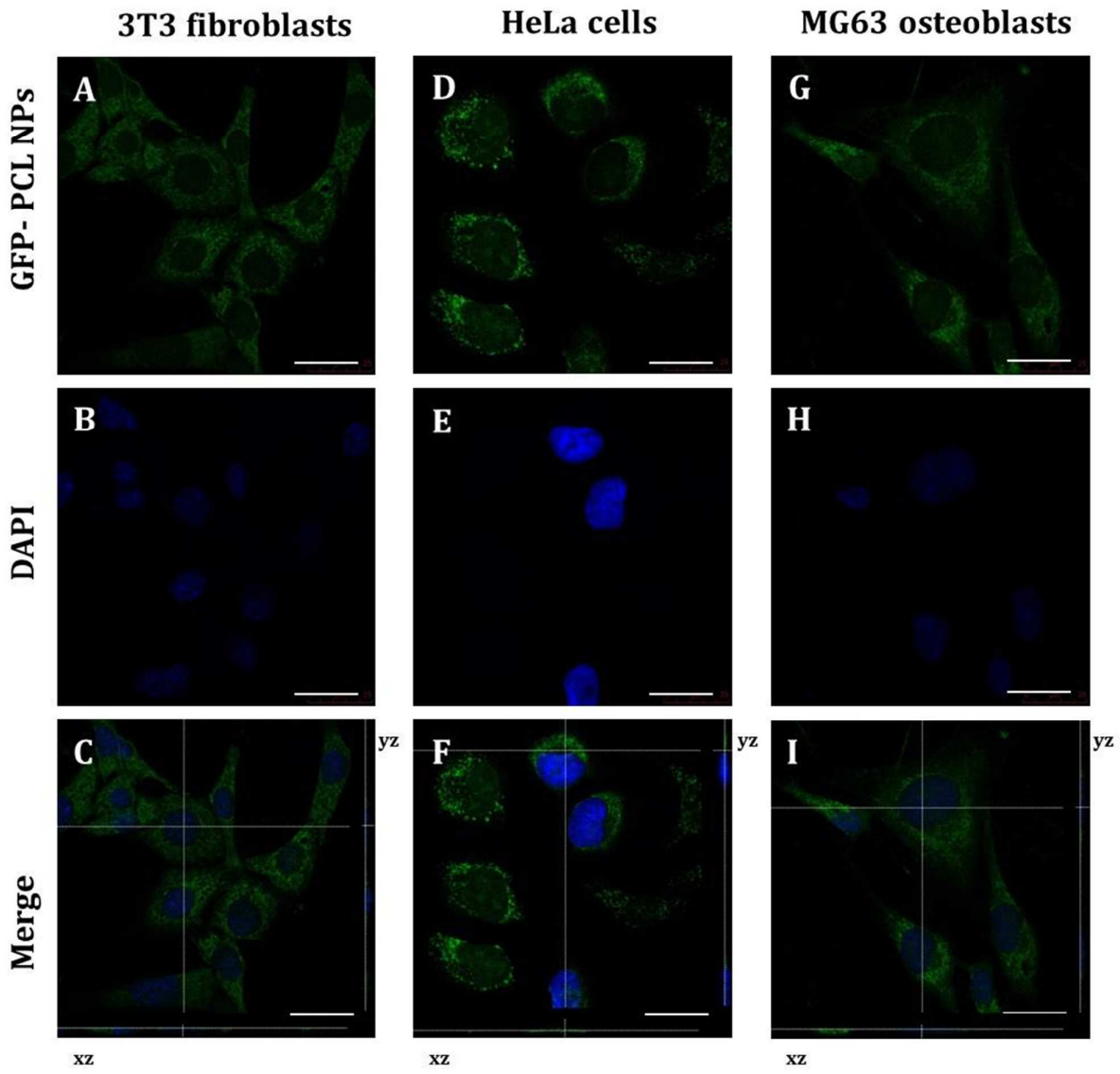

Fig. 5. CLSM images of GFP-mRNA expression delivered by PCL NPs of the transfected NIH 3T3 fibroblasts(A,B,C), HeLa cells (D,E,F) and MG63 osteoblasts (G,H,I) after 24 hours of incubation. CLSM images A,D,G shown the expression of GFP (green). Cell nuclei were counterstained with DAPI (blue) as shown in the CLSM images B,E,H. Each merge of confocal images (C,F,I) reports the corresponding Z-stack optical sections (yz and xz) obtained through photoluminescence reconstruction in the z-direction, with a z-resolution of 200 nm to confirm the spatial GFP expression inside cells. *Scale bars: 25 µm.*

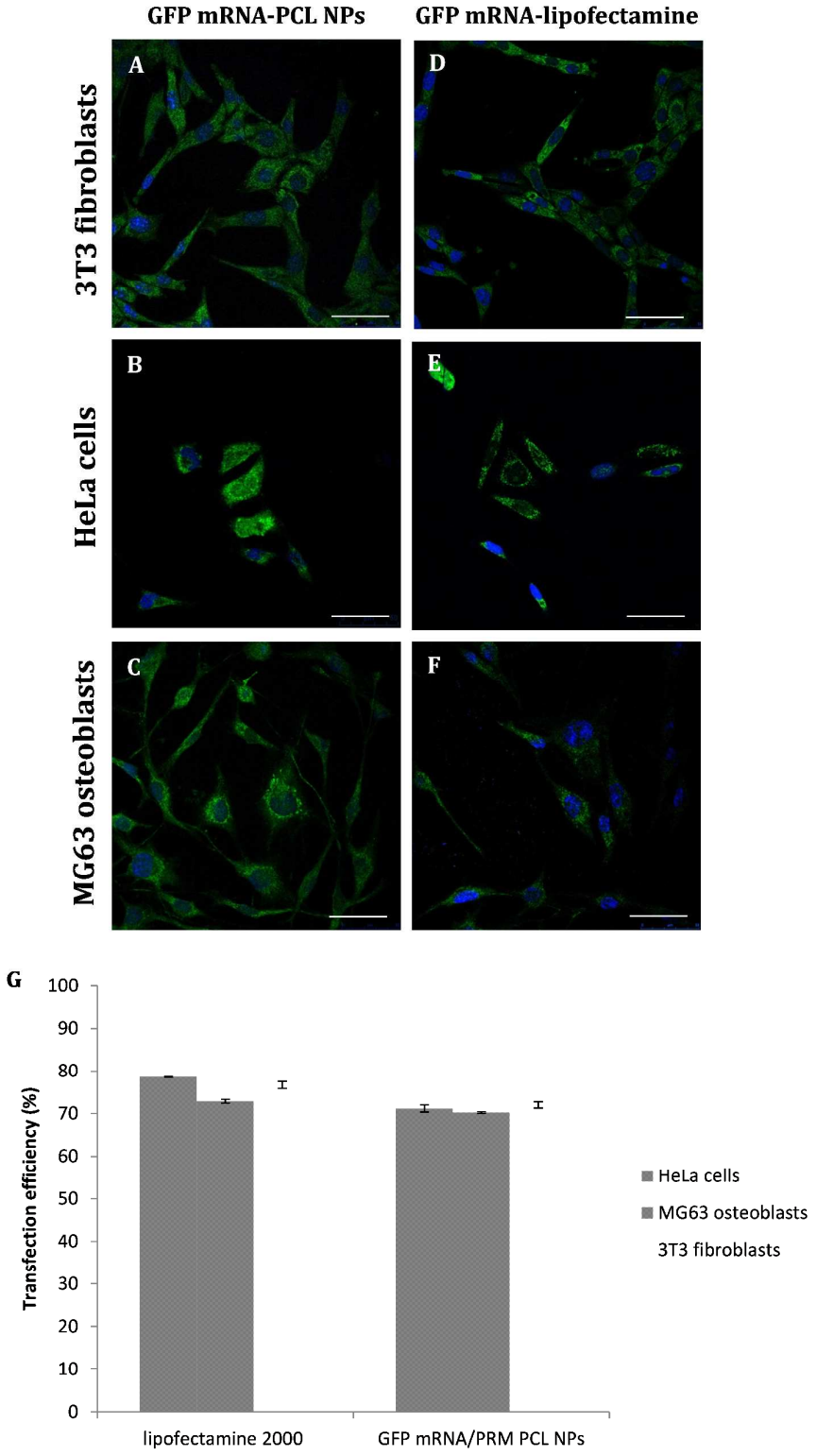

Fig. 6. CLSM images of differential GFP-mRNA expression (green) delivered by PCL NPs (A,B,C) and Lipofectamine 2000 (C,D,E) of the transfected NIH 3T3 fibroblasts (A,D), HeLa cells (B,E) and MG63 osteoblasts (C,F) after 24 hours of incubation. Cell nuclei were counterstained with DAPI (blue). *Scale bars: 50 μm*. (G) Transfection efficiency (%) of mRNA-GFP delivery by PCL NPs or Lipofectamine 2000. Representative measurements of three distinct sets of data have been reported (*t-Student test, $P < 0.05$*).

GFP mRNA-protamine complexes encapsulated poly (ε-caprolactone) (PCL) non-viral nanoparticles are proposed for the intracellular delivery of mRNA molecules.

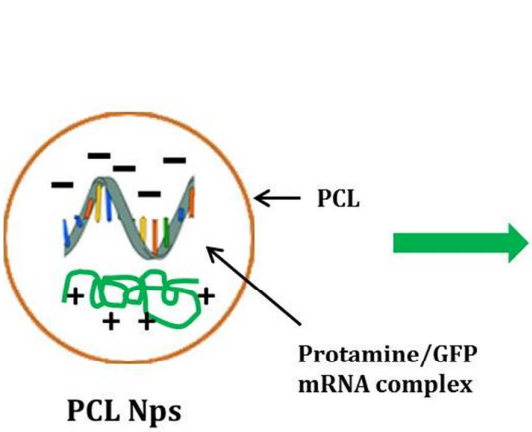

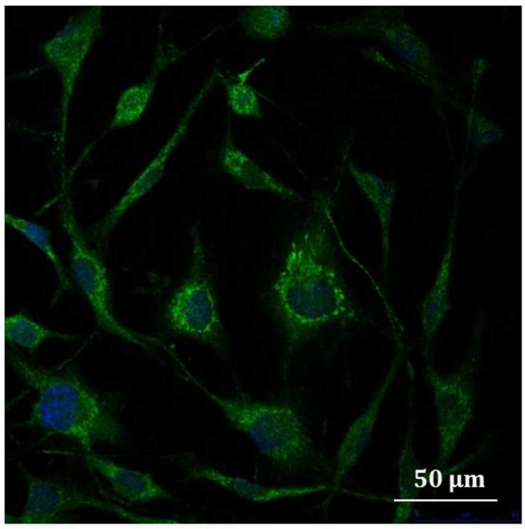

Osteoblasts expressing GFP (green) after transfection with non-viral delivery of GFP mRNA loaded PCL nanoparticles.